CHIN. PHYS. LETT. Vol. 35, No. 11 (2018) 116301

Coherent Acoustic Phonon and Its Chirping in Dirac Semimetal Cd_3As_2 *

Fei Sun(孙飞)[1,2†], M. Yang(杨萌)[1,2†], M. W. Yang(杨明卫)[1,2], Q. Wu(吴穹)[1,2], H. Zhao(赵惠)[1,2], X. Ye(叶霞)[1,2], Youguo Shi(石友国)[1,2], Jimin Zhao(赵继民)[1,2**]

[1]*Beijing National Laboratory for Condensed Matter Physics, Institute of Physics, Chinese Academy of Sciences, Beijing 100190*

[2]*School of Physical Sciences, University of Chinese Academy of Sciences, Beijing 100049*

(Received 24 September 2018)

Ultrafast optical spectroscopy of a single crystal of a Dirac semimetal Cd_3As_2 is carried out. An acoustic phonon (AP) mode with central frequency $f = 0.037$ THz (i.e., 1.23 cm^{-1} or 0.153 meV) is unambiguously generated and detected, which we attribute to laser-induced thermal strain. An AP chirping (i.e., variation of the phonon frequency) is clearly detected, which is ascribed to heat capacity variation with time. By comparing our experimental results and the theoretical model, we obtain a chirping time constant, which is 31.2 ps at 6 K and 19.8 ps at 300 K, respectively. Significantly, we identify an asymmetry in the AP frequency domain peak and find that it is caused by the chirping, instead of a Fano resonance. Moreover, we experimentally demonstrate that the central frequency of AP is extremely stable with varying laser fluence, as well as temperature, which endows Cd_3As_2 application potentials in thermoelectric devices.

PACS: 63.20.−e, 78.47.D−, 78.47.−p, 71.55.Ak DOI: 10.1088/0256-307X/35/11/116301

Topological quantum materials have recently attracted enormous research interests owing to their non-trivial electronic structures in momentum space, as well as potential applications in electronics and photonics devices. The theoretical predictions[1,2] and concomitant experimental investigations[3−6] of Dirac semimetal Cd_3As_2 is a milestone in the development of topological quantum states. Early investigations focused mainly on the electronic,[4,7] magnetic[5] and transport properties.[6] Recently, theoretical investigations predicted novel interactions between the topological electronic states and lattices.[8−11] However, so far there are relatively few experimental investigations in the lattice degree of freedom for topological quantum materials.[12,13]

Here we report an ultrafast optical pump-probe spectroscopy investigation of Cd_3As_2, ranging from liquid helium temperature to room temperature. Besides observing the relaxation process of photo-excited carriers, a coherent acoustic phonon (AP) mode has also been generated and detected, which we attribute to a thermal strain wave origin. Furthermore, a frequency chirping of the AP mode is observed. We also find an asymmetry of the AP in the frequency domain. Our analysis shows that the asymmetry is caused by its chirping, instead of a Fano resonance. By measuring the temperature dependence, we identify that the AP chirping decays exponentially with increasing temperature. In addition, a coherent A_{1g} optical phonon mode with a frequency of 0.69 THz (i.e., 23 cm^{-1} or 2.85 meV) has also been observed.

In our experiment, a Ti:sapphire re-generative amplifier is used, where the experimental setup is similar to that given in Ref. [12]. The ultrafast laser pulse has an 800 nm central wavelength, 70 fs pulse duration and 250 kHz repetition rate. The pump and probe beams spatially overlap on the Cd_3As_2 sample (010) surface, and the time delay between the pump and probe beams is scanned. The differential reflectivity $\Delta R(t)$ is collected by a photodiode, modulated by a mechanical chopper at 2.1 kHz, and sampled by a lock-in amplifier to enhance the signal-to-noise ratio. During the temperature dependence measurements, the pump and probe fluences are kept at 3.4 mJ/cm^2 and 1.3 mJ/cm^2, respectively. Details of our sample preparation were reported in Ref. [5].

In Fig. 1(a), we show a typical result of the ultrafast dynamics of Cd_3As_2 at 6 K. The relative differential reflectivity of the probe beam, $\Delta R/R_0$, is recorded as a function of the delay time between the pump and probe pulses. The pump photon has an energy of 1.55 eV, which promotes the valance electrons to an excited state that is far above the Dirac point. The relaxation process of photo-induced carriers is complex, consisting of sub-picosecond electron-electron scattering, picosecond electron-phonon scattering, slower phonon-phonon scattering and subsequent thermalization. After the excitation, $\Delta R/R_0$ exhibits a rapid relaxation process followed by one or more concomitant slow relaxation processes of opposite sign. We fit the results using the equation

$$\Delta R/R_0 = A_{\rm fast}e^{-t/\tau_{\rm fast}} + A_{\rm slow1}e^{-t/\tau_{\rm slow1}} + A_{\rm slow2}e^{-t/\tau_{\rm slow2}}, \quad (1)$$

*Supported by the National Key Research and Development Program of China under Grant Nos 2017YFA0303603, 2016YFA0300303, 2017YFA0302901 and 2016YFA0300604, the National Natural Science Foundation of China under Grant Nos 11774408, 11574383 and 11774399, the External Cooperation Program of Chinese Academy of Sciences under Grant No GJHZ1826, and the Interdisciplinary Innovation Team of Chinese Academy of Sciences.

†These authors contributed equally.

**Corresponding author. Email: jmzhao@iphy.ac.cn

© 2018 Chinese Physical Society and IOP Publishing Ltd

where $\tau_{\rm fast}$, $\tau_{\rm slow1}$ and $\tau_{\rm slow2}$ are the lifetimes of the relaxation processes, $A_{\rm fast}$, $A_{\rm slow1}$ and $A_{\rm slow2}$ are the corresponding amplitudes.

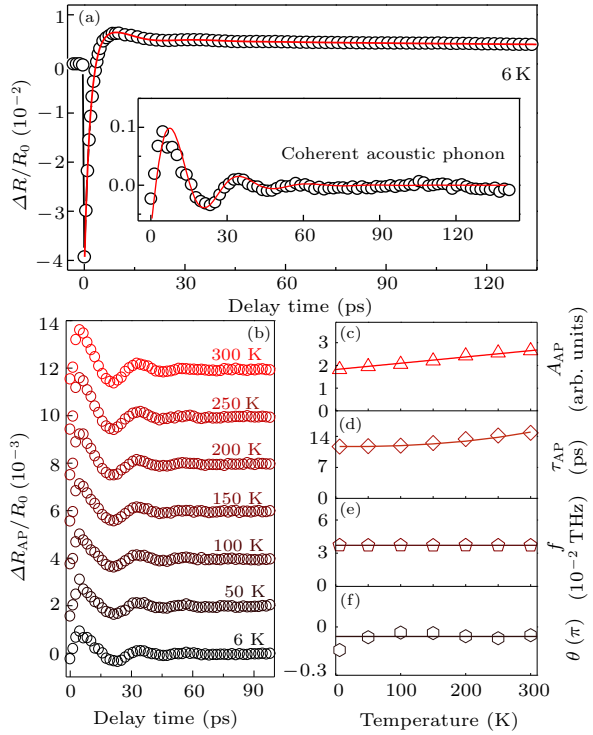

Fig. 1. (a) Relative differential reflectivity $\Delta R/R_0$ at 6 K, with a red fitting curve. Inset: AP oscillation after subtracting the quasiparticle dynamics from the scanning trace. (b) Coherent AP at a few typical temperatures ranging from 6 K to 300 K. (c)–(f) Fitting parameters of the AP: amplitude (c), lifetime (d), frequency (e), and initial phase (f). Solid curves: guides to the eyes.

Notably, other than the quasiparticle dynamics described by the above three relaxation processes, a periodic damping oscillation is also clearly identified, superimposed on the $\Delta R/R_0$ trace, which we attribute to a coherent AP.[14–18] To focus on the AP, we extract the oscillation by subtracting the electronic dynamics from $\Delta R/R_0$. We explicitly plot the oscillation at 6 K in the inset of Fig. 1(a). The oscillation can be fitted by the following equation

$$\Delta R_{\rm AP}/R_0 = A_{\rm AP} e^{-t/\tau_{\rm AP}} \sin(2\pi f t + \theta), \qquad (2)$$

where $A_{\rm AP}$, $\tau_{\rm AP}$, f and θ represent the amplitude, lifetime, central frequency and initial phase of the AP, respectively. As shown in the inset of Fig. 1(a), the experimental result at 6 K (black circles) is fitted by Eq. (2) (red curve). In Fig. 1(b), we show the AP at a few typical temperatures 6 K, 50 K, 100 K, 150 K, 200 K, 250 K and 300 K, respectively. Complete information about the parameters of the AP is obtained by fitting the temperature-dependent data using Eq. (2). In Figs. 1(c)–1(f) we show the temperature dependence of all these parameters: amplitude, frequency, lifetime and initial phase. It can be seen that the amplitude increases linearly with temperature, the lifetime increases nonlinearly with temperature, the central frequency (0.037 THz, i.e., 0.153 meV or 1.23 $\rm cm^{-1}$) and the initial phase (-0.1π) stay constant with temperature.

Under the pump pulse excitation, the sample surface absorbs the light energy and is then heated. The ultrafast heating generates a transient temperature rise and a thermal strain pulse propagating along the longitudinal direction, which excites an acoustic wave.[19,20] Note that the sample is thick (>100 μm) enough to rule out the possibility of a standing acoustic wave formed along the propagating direction. Owing to the thermal strain wave origin, the frequency of the AP does not depend on the sample thickness, as demonstrated by Fig. S1(a) in the Supplementary Materials.

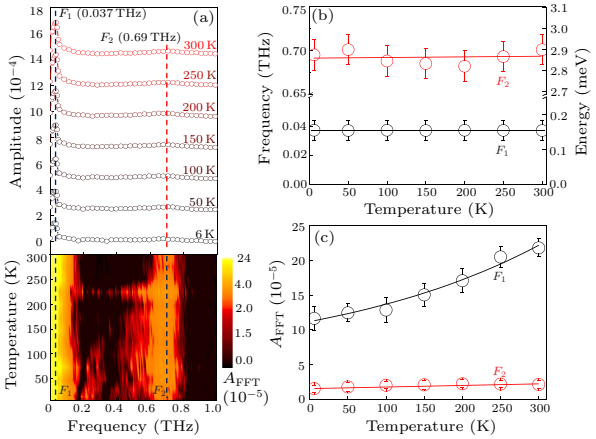

Fig. 2. (a) Temperature dependence of the FFT of the time domain phonon oscillations. Here F_1 and F_2 mark the AP and optical phonon modes, respectively. Bottom panel: color mapping of the results in upper panel. Two peaks, marked by yellow and erythrine stripes, can be identified. Temperature dependence of their frequency (b) and amplitude (c) are shown. Dashed lines in (a) and solid curves in (b) and (c): guides to the eyes.

To fully understand the AP, we investigate it in the frequency domain. In the upper panel of Fig. 2(a), the fast Fourier transformation (FFT) results of the AP are plotted (data offset for clarity). The AP mode at 0.037 THz (marked by F_1) can be clearly identified. Also observable is another much weaker and broader peak at 0.69 THz (marked by F_2). Our experimental geometry allows for the A_{1g} and B_{1g} phonon symmetries,[12,21] and the wavenumber of F_2 mode is consistent with the Raman scattering results of an A_{1g} optical phonon mode.[22] Thus we attribute F_2 to an A_{1g} optical phonon mode. The broader peak indicates that its lifetime is much shorter, hardly discernible in time domain. To vividly depict the FFT results, we also color-map the FFT spectrum in the lower panel of Fig. 2(a). A yellow stripe corresponding to the F_1 peak is revealed, as well as an erythrine stripe for the F_2 peak. The temperature dependence of the frequency is plotted in Fig. 2(b), which does not change with temperature, as in the time domain result in Fig. 1(e). The temperature dependence of the FFT amplitude is plotted in Fig. 2(c), which significantly

increases with temperature. As shown in Ref. [12], the amplitude in frequency domain is proportional to the product of the time domain amplitude and lifetime. Thus as is expected, the results in Fig. 2(c) is also consistent with that in Figs. 1(c) and 1(d). For the F_2 optical phonon peak, the frequency and amplitude do not change with temperature.

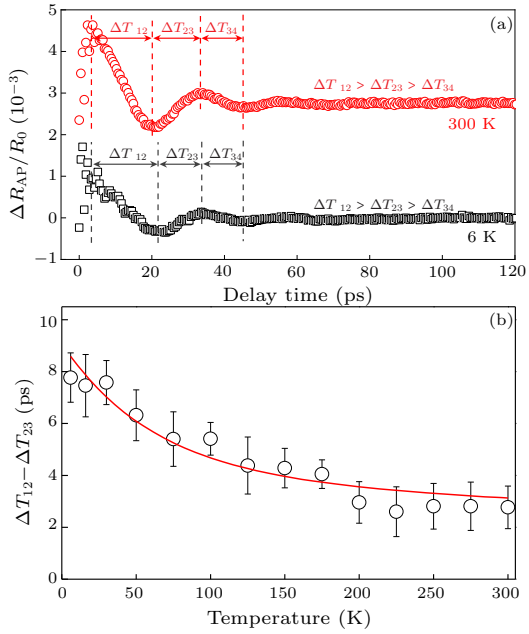

Fig. 3. AP chirping represented by $\Delta T_{12} - \Delta T_{23}$. (a) The chirping $\Delta T_{12} - \Delta T_{23}$ is larger at 6 K than at 300 K, (b) $\Delta T_{12} - \Delta T_{23}$ varies with temperature. The red curve is an exponential fitting curve.

Significantly, a chirping (i.e., the frequency changes with time) in the AP oscillation can be identified. We replot the time domain AP oscillation in Fig. 3(a), and compare its first, second, and third half periods. The varying period, $\Delta T_{12} > \Delta T_{23} > \Delta T_{34}$, corresponds to a time-varying frequency (i.e., chirping), which is more pronounced at a low temperature (Fig. 3(a)). Such an AP chirping phenomenon is not very common, because in many materials the AP frequency is a constant.[14,15,23–27]

Next, we consider the temperature dependence of the chirping property. We use $\Delta T_{12} - \Delta T_{23}$ to represent the chirping magnitude and plot its temperature dependence in Fig. 3(b). It can be fitted well by an exponential decay function (red curve). As shown, the chirping is more pronounced at lower temperatures. We speculate that this is because the transient change of heat capacity during the AP propagation is larger at lower temperatures (see the following discussion related to Fig. 5).

To understand the AP chirping, we revise Eq. (2) by introducing a time-dependent frequency to account for the chirping. As a natural starting choice, we incorporate a chirping that decays exponentially with time. Explicitly,

$$\Delta R_{AP}/R_0 = A_{AP} e^{-t/\tau_{AP}} \sin(2\pi f(1-\xi e^{-t/\tau_\alpha})t - \theta), \quad (3)$$

where we define τ_α to be the chirping time constant of the AP, and ξ to be the chirping magnitude.

Interestingly, careful observation of the frequency domain AP peak (Fig. 2(a)) reveals a clear asymmetric line shape, which we replot in Fig. 4. In Fig. 4(a), the temperature dependence of the normalized FFT amplitude is shown, demonstrating an increasing asymmetry with decreasing temperature. To see this clearly, we compare the 6 K and 300 K results in Fig. 4(b). It can be seen that the peak asymmetry is more prominent at 6 K. Phonon peak asymmetry is most commonly observed as a result of Fano resonance.[28] However, here we contemplate that the AP asymmetry observed is due to the AP chirping, instead of a Fano resonance. In general, Fano resonance is due to the coupling between a continuum state (usually metallic states) and a discrete state (here, the AP). In semimetal Cd_3As_2, there is no metallic state reported.[5,6] Thus it is unlikely that Fano resonance can exist. As evidence, the optical phonon modes previously observed do not exhibit an asymmetric line shape[12] (i.e., no Fano asymmetry), demonstrating the lack of a continuum state.

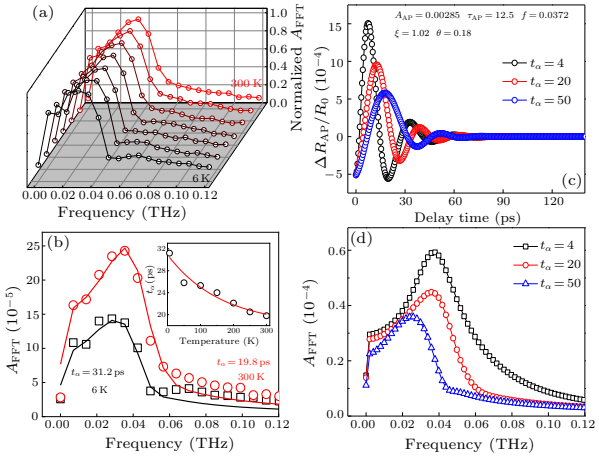

Fig. 4. (a) Temperature dependence of normalized A_{FFT}. (b) Comparison of the frequency peaks at 6 K and 300 K. Solid curves: fitting curves based on Eq. (3). The asymmetry of the peak is more pronounced at a lower temperature. Inset: temperature dependence of τ_α, with a fitting of a red exponential curve. (c) Simulations of the AP with chirping, where $A_{AP} = 0.00285$, $\tau_{AP} = 12.5$ ps, $f = 0.0372$ THz, $\xi = 1.02$, $\theta = 0.18$, and $\tau_\alpha = 4$, 20, and 50 ps, respectively. (d) Corresponding FFT results of the simulated oscillations in (c).

To verify whether chirping causes the asymmetry, we numerically simulate the AP chirping based on Eq. (3). The simulation results in time domain and their FFT results in frequency domain are displayed in Figs. 4(c) and 4(d), respectively. In each figure, three curves are plotted, with τ_α being 4, 20 and 50 ps, respectively. The value of ξ is chosen arbitrarily to be 1.02. Indeed we have also tried to assign ξ to be 1, which yields very similar results. In Fig. 4(c), for the blue curve, the chirping time constant τ_α is larger, of which the curve shape is similar to the low temperature case in Fig. 3(a). Thus larger τ_α corresponds

to the lower temperature case, which exhibits more prominent AP asymmetry.

Note in Fig. 4(b), in each of the curves, the second experimental data point (square or circle) is not tightly connected with the first data point. There is a finite value difference between them. Such a value difference is not noise, but clear experimental results. Interestingly, in the simulation results shown in Fig. 4(d), this finite value difference can also be identified clearly. To see whether the simulation results compare well with the experimental results, we plot them together in Fig. 4(b) (black and red solid curves). It can be seen that the curves overall fit the experimental results very well. By optimizing the simulation, the AP chirping time constant τ_α is obtained to be 31.2 ps at 6 K and 19.8 ps at 300 K. The comprehensive temperature dependence of τ_α is shown in the inset of Fig. 4(b), taking into account results for different temperatures not explicitly shown in Fig. 4(b). It can be seen that τ_α decreases exponentially with temperature. Our results in Fig. 4 demonstrate that a pure chirping oscillation can reproduce the peak asymmetry in frequency domain. Thus we conclude that the AP asymmetry we observe can be well explained simply by chirping. With the discussion on continuum state in the earlier paragraph, we conclude that the asymmetry we observe is caused by chirping, instead of Fano resonance. Note that, as discussed in the Supplementary Materials (see Fig. S2), the chirping we observe here is unlikely an inevitable artifact due to the subtraction of the electronic dynamics. Even if we analyze the data by starting from different scanning points, the asymmetry always exists.

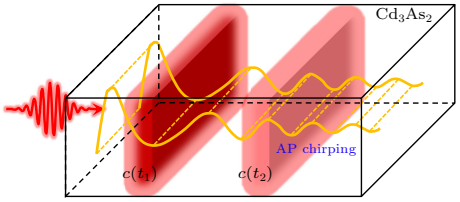

Fig. 5. The chirping mechanism for AP. Dark and light red cuboids represent large ($c(t_1)$) and small ($c(t_2)$) transient heat capacities, respectively, as a result of temperature change. The gold curve depicts the AP with chirping.

We discuss the underlying mechanism of the chirping. Nonetheless, AP chirping has been observed in a number of materials, including Ge, Si, quartz, GaAs, etc.[29–31] Nonlinear dispersion of AP has been considered to explain the chirping,[29–31] whereas the heating effect on the material due to the ultrafast light pulses has not been taken into account. In Fig. 5, we schematically illustrate the generation mechanism of the AP chirping in our case. After the ultrafast optical pulse excitation, AP is generated. During the propagation of AP, the temperature decreases with time and location, leading to varying heat capacity with location. Larger ($c(t_1)$) and smaller ($c(t_2)$) heat capacities are marked by dark and light red cuboids, respectively, in Fig. 5. As a result, different heat capacities lead to different frequencies, thus exhibiting a chirping in the AP. Indeed, the fact that $\xi = 1$ in Eq. (3) is fully consistent with the physics picture discussed here. That is, the chirping is caused during the propagation of the AP wave. Both the generation and the chirping is of thermal origin, thus no extra physical origin needs to be introduced.

In addition, we systematically investigate the laser fluence dependence of the AP. The results at 6 K and 300 K are shown in Fig. 6. It can be seen that the AP amplitude increases linearly with the laser fluence. Explicitly, we show it in the insets, indicating that there is no saturation observed even for a laser fluence as high as 5.5 mJ/cm^2. We further show in Fig. S1 (see Supplementary Materials) that the central frequency of the AP does not vary with laser fluence either. Such exceptionally sturdy optical and thermal properties might be useful in the future applications of thermoelectric devices.

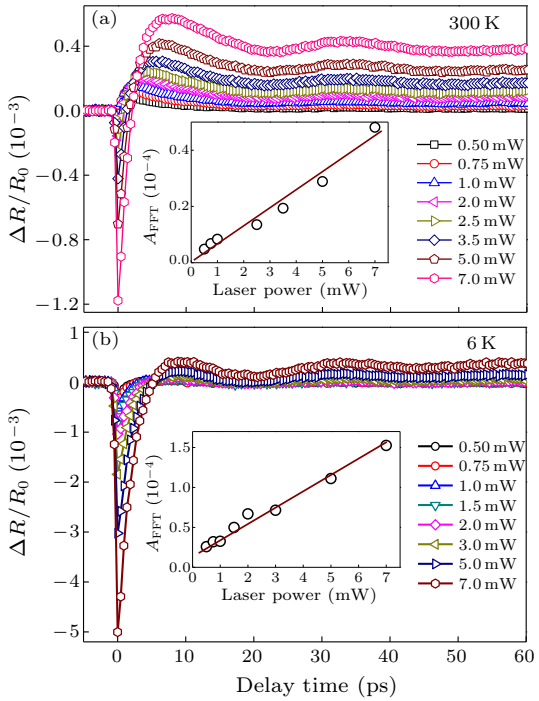

Fig. 6. Excitation pump power dependence of $\Delta R/R_0$ at 300 K (a) and 6 K (b), respectively. The insets show the power dependences of $A_{\rm FFT}$ of the AP. Linear dependences are identified (wine lines, guide to the eyes), without sign of saturation.

In summary, coherent AP in a Dirac semimetal crystal Cd_3As_2 is generated and detected, with a central frequency of 0.037 THz, which we attribute to thermal strain wave origin. A chirping of the AP is clearly observed in time domain and an asymmetry line shape in frequency domain is also identified. We attribute the chirping mechanism to be transient heat capacity change. Significantly, our investigations, including a simulation, demonstrate that the asymmetry in the FFT peak is caused by the AP chirping, instead of a Fano resonance. This conclusion is qualitatively consistent with our temperature dependence investi-

gation, where chirping exhibits an exponential decay with increasing temperature. In addition, we demonstrate that the central frequency of the AP does not vary with laser fluence and temperature, facilitating thermoelectric device applications.

References

[1] Wang Z J, Weng H M, Wu Q S et al 2013 *Phys. Rev.* B **88** 125427
[2] Young S M, Zaheer S, Teo J C Y et al 2012 *Phys. Rev. Lett.* **108** 140405
[3] Borisenko S, Gibson Q, Evtushinsky D et al 2014 *Phys. Rev. Lett.* **113** 027603
[4] Yi H M, Wang Z J, Chen C Y et al 2015 *Sci. Rep.* **4** 6106
[5] Feng J Y, Pang Y, Wu D S et al 2015 *Phys. Rev.* B **92** 081306(R)
[6] He L P, Hong X C, Dong J K et al 2014 *Phys. Rev. Lett.* **113** 246402
[7] Lv B Q, Weng H M, Fu B B et al 2015 *Phys. Rev.* X **5** 031013
[8] Song Z D, Zhao J M, Fang Z et al 2016 *Phys. Rev.* B **94** 214306
[9] Rinkel P, Lopes P L S and Carate I 2017 *Phys. Rev. Lett.* **119** 107401
[10] Pikulin D I, Chen A and Franz M 2016 *Phys. Rev.* X **6** 041021
[11] Cortijo A, Ferreirós Y, Landsteiner K et al 2015 *Phys. Rev. Lett.* **115** 177202
[12] Sun F, Wu Q, Wu Y L et al 2017 *Phys. Rev.* B **95** 235108
[13] Kumar N, Ruzicka B A, Butch N P et al 2011 *Phys. Rev.* B **83** 235306
[14] Tian Y C, Zhang W H, Li F S et al 2016 *Phys. Rev. Lett.* **116** 107001
[15] Ren Y H, Lupke C, Hu Y F et al 2006 *Phys. Rev.* B **74** 012405
[16] Zhang X, Qiao X F, Shi W et al 2015 *Chem. Soc. Rev.* **44** 2757
[17] Merlin R 1997 *Solid State Commun.* **102** 207
[18] Li J J, Chen J, Reis D A et al 2013 *Phys. Rev. Lett.* **110** 047401
[19] Sheu Y M, Chien Y J, Uher C et al 2013 *Phys. Rev.* B **87** 075429
[20] Thomsen C, Grahn H T, Maris H J et al 1986 *Phys. Rev.* B **34** 4129
[21] Liu Z H, Lu X X, Peng P et al 2010 *Phys. Rev.* B **82** 155435
[22] Weszka J 1999 *Phys. Stat. Sol.* (b) **211** 605
[23] Ge S F, Liu X F, Qiao X F et al 2014 *Sci. Rep.* **4** 5722
[24] Zhao J M, Bragas A V, Lockwood D J et al 2004 *Phys. Rev. Lett.* **93** 107203
[25] Bragas A V, Aku-Leh C, Costantino S et al 2004 *Phys. Rev.* B **69** 205306
[26] Aku-Leh C, Zhao J, Merlin R et al 2005 *Phys. Rev.* B **71** 205211
[27] Zhao J M, Bragas A V and Merlin R 2006 *Phys. Rev.* B **73** 184434
[28] Zhao J M 2005 *Ultrafast Optical Generation of Squeezed Magnon States and Long Lifetime Coherent LO Phonons* (The University of Michigan: Phd Dissertation)
[29] Hao H Y and Maris H J 2000 *Phys. Rev. Lett.* **84** 5556
[30] Hao H Y and Maris H J 2001 *Phys. Rev.* B **63** 224301
[31] Poyser C L, York W B, Srikanthreddy D et al 2017 *Phys. Rev. Lett.* **119** 255502

Supplementary Materials: Coherent Acoustic Phonon and Its Chirping in Dirac Semimetal Cd_3As_2*

Fei Sun(孙飞) [1,2,†], M. Yang(杨萌) [1,2,†], M. W. Yang(杨明卫) [1,2], Q. Wu(吴穹) [1,2], H. Zhao(赵惠) [1,2], X. Ye(叶霞) [1,2], Y. G. Shi(石友国) [1,2], Jimin Zhao(赵继民) [1,2**]

Coherent AP in different Samples

If the AP is a standing wave in the crystal, the frequency will vary with the thickness of the sample. Here, in order to verify on this, we conduct the same ultrafast measurements on different samples (labelled by Sample 1 and Sample 2) of different thickness. As shown in Fig. S1(a), the AP in these two samples exhibits identical frequency. Note that all the data mentioned in the main text are collected in Sample 1 except Fig. 6. In Fig. 6 of the main text, we show the results of pump power dependence investigation on Sample 2. Furthermore, we demonstrate the pump power dependence of the AP frequency in Fig. S1(b). It can be seen that the frequency stays constant with pump power, whether at 6 K or 300 K.

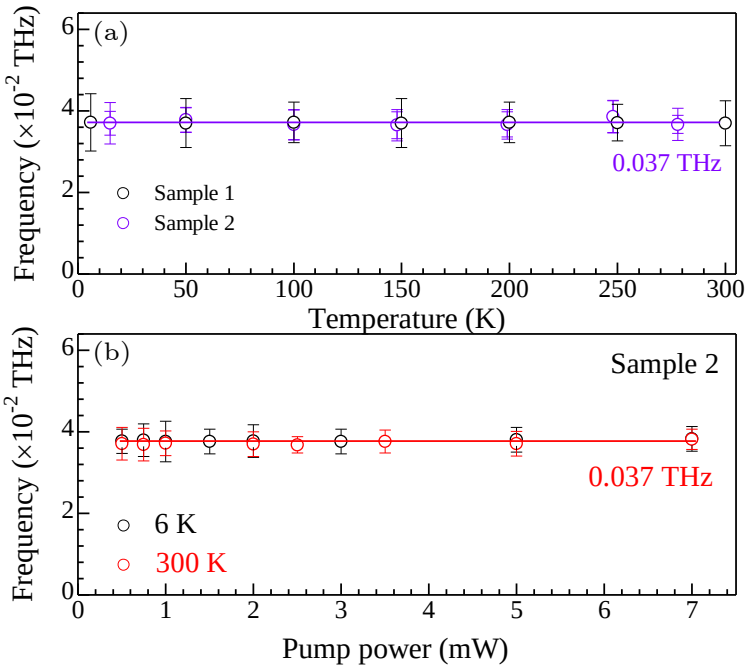

Fig. S1. (a) Comparing the AP frequency between different samples with different thicknesses. (b) Pump power dependence of the AP frequency in Sample 2 at 6 K and 300 K, respectively. The frequency (0.037 THz) is nearly independent of pump power.

Confirmation of the existence of AP chirping

In order to rule out the possibility that the AP chirping is an artifact due to the subtraction of the electronic dynamics. We analyze the asymmetry of the frequency peak for different cases with different starting time t_0 in time domain (at 6 K). In Fig. S2(a), we show the time domain oscillations with different starting times t_0. In Fig. S2(b), we show the corresponding FFT results. It can be seen from Fig. S2(b) that the asymmetric line-shape always exists for different cases of different t_0. Thus, our analysis demonstrates that the AP chirping is independent of the choice of the starting time. This basically rules out the potential "artifact alternative" for the chirping.

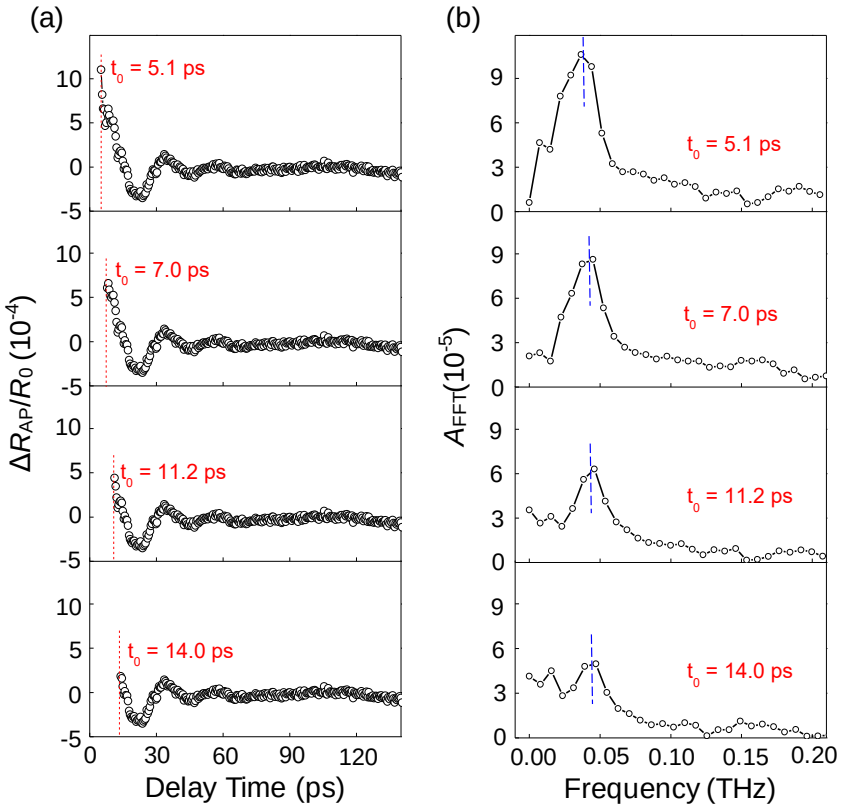

Fig. S2. Discussion and verification on the potential "artifact alternative" for the chirping. (a) The AP time domain oscillations with different starting time t_0. (b) The corresponding FFT results in frequency domain. All these data are collected at 6 K. Asymmetry can be identified in all figures of (b), although the starting time t_0 is different.